Discharge and location dependency of calibrated main channel roughness: case study on the River Waal and IJssel

B.C.A. Domhof[1], K.D. Berends[1,2], A. Spruyt[2], J.J. Warmink[1], S.J.M.H. Hulscher[1]

[1] *University of Twente, Enschede, Netherlands*

[2] *Deltares, Delft, Netherlands*

ABSTRACT: To accurately predict water levels, river models require appropriate description of the hydraulic roughness. The bed roughness increases as river dunes grow with increasing discharge and the roughness depends on differences in main channel and floodplain width and bed sediment. Therefore, we hypothesize that the calibrated main channel roughness coefficient is most sensitive to the discharge and location in longitudinal direction of the river. The roughness is determined by calibrating the Manning coefficient of the main channel in a 1D hydrodynamic model. The River Waal and IJssel in the Netherlands are used as case studies. Results show that the calibrated roughness is mainly sensitive to discharge. Especially the transition from bankfull to flood stage, effects of floodplain compartmentation and bankfull overflow in sharp bends are important features to consider in the calibration. Capturing these features in the calibration produce more accurate water level predictions. Moreover, the downstream boundary condition also has a large effect on the calibrated roughness values near the downstream boundary.

1 INTRODUCTION

Hydrodynamic river models are used to predict water levels along the river and support decision making in river management. The models are used to monitor the river and to study the effects of measures in the river to decrease the risk of flooding in high water situations and prevent drought in low water situations. Therefore, the model predictions need to be sufficiently accurate. Insufficiently accurate predictions may, for example, lead to the construction of dikes which are too low which in turn can lead to major damages and casualties in case of flooding.

Hydrodynamic models are calibrated and validated to increase accuracy. Calibration involves minimizing the errors between the predictions and observations by altering model parameters. Validation involves verifying whether the calibrated model parameters also produce minimal errors between predictions and observations in different models. In most calibration studies of hydrodynamic models, the hydraulic roughness coefficient is calibrated because it is the most uncertain parameter (Bates et al., 2004; Hall et al., 2005; Pappenberger et al., 2005; Vidal et al., 2007; Warmink et al., 2011). Furthermore, this coefficient is often treated as a dustbin parameter to compensate for all kinds of model errors, by for example simplifying the river bathymetry into a limited number of cross-sections (Morvan et al., 2008).

Both the physical and calibrated bed roughness can vary along the longitudinal direction of the river due to differences in main channel and floodplain width and bed sediment. Moreover, the floodplain vegetation influences the compound roughness during flood discharge stage. Furthermore, Julien et al. (2002) shows that as discharge increases, river dunes grow in the main channel leading to an increasing bed roughness. Best (2005) argues that river dunes are present in nearly all river systems.

Therefore, it is hypothesized that the calibrated hydraulic roughness is mostly sensitive to the discharge and location in longitudinal direction of the river. The calibration study of Warmink et al. (2007) confirms this hypothesis. However, this study does not explain why and how the calibrated roughness varies along the longitudinal direction of the river and the discharge stages.

In this study we answer the research questions: 1) why and how the calibrated roughness varies along the longitudinal direction of the river and discharge stage, and 2) what the sensitivity of water level prediction accuracy to these variations is. We use a case study on the River Waal and on the River IJssel in The Netherlands.

The main objective in this study is to investigate the location and discharge dependency of the main channel roughness by calibration. Validation is performed to check if the calibrated roughness also results in accurate water level predictions. The conclusions of this study can help to improve the water level prediction accuracy of 1D hydrodynamic models.

Chapter 2 presents a description of the River Waal and IJssel. Chapter 3 presents the method and chapter 4 presents the calibrated roughness values. Chapter 5 shows the validation results using the calibrated roughness values. Finally, chapter 6 presents a discussion and chapter 7 the conclusion of this study.

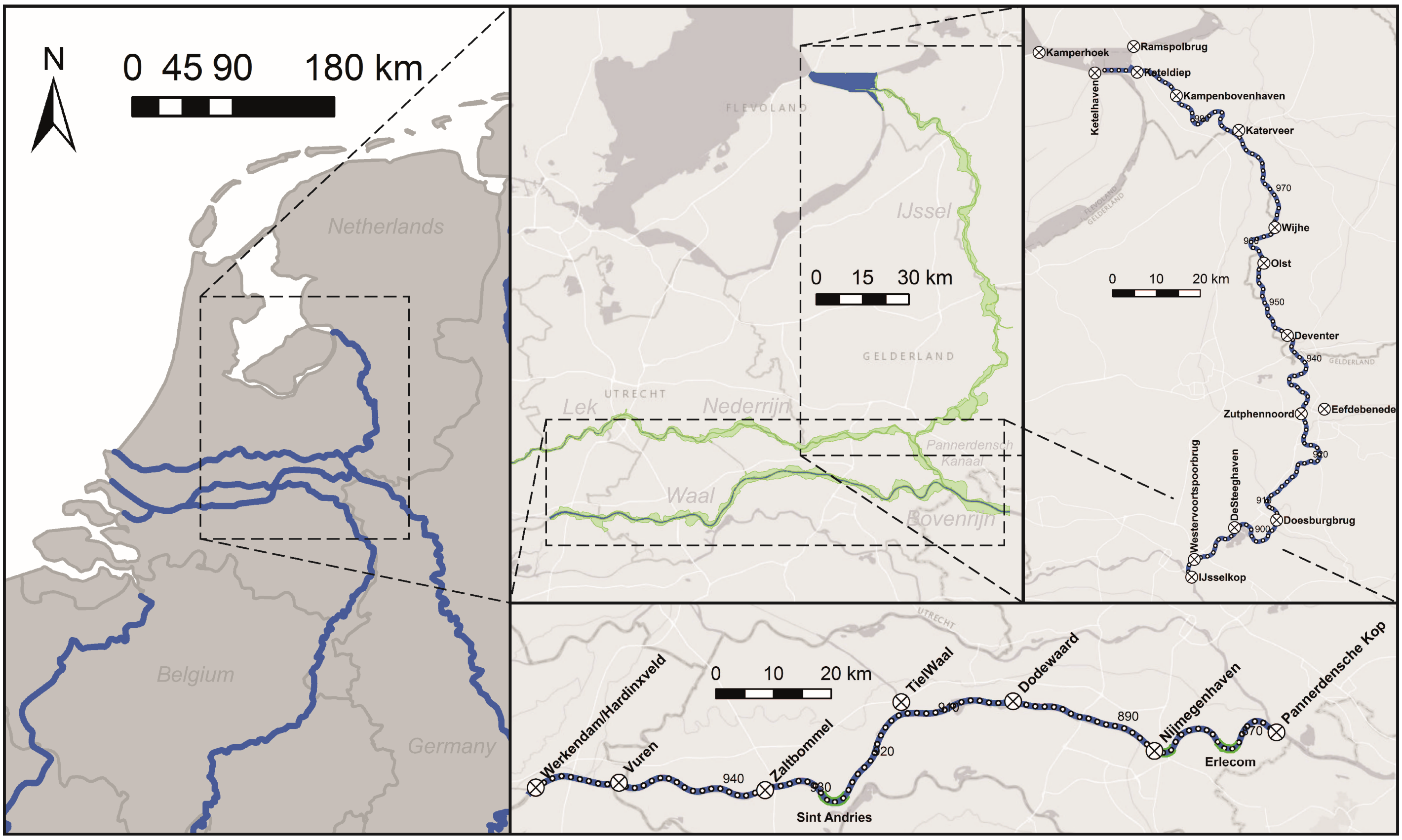

Figure 1. Geographic overview of the River Waal (lower right panel) and IJssel (upper right panel) in the Netherlands. Round crossed circles indicate observation station locations. Small white points along the river length are one kilometer spaced apart. Green highlighted river section in bends of the Waal indicate the location of submerged groynes and artificial armoured bed layers.

2 STUDY AREA

2.1 *River Waal*

The lower right panel in Figure 1 presents a geographical overview of the River Waal. The Waal is a distributary of the River Rhine in the Netherlands. The Rhine bifurcates at the Pannerdensche Kop into the Pannerdensch Kanaal and the Waal. The Waal bifurcates at the end into the Beneden-Merwede and Nieuwe Merwede. The latter flows into the estuary Hollands Diep. Therefore, tidal influences at the downstream boundary of the Waal are present.

Along the Waal, seven water level observation stations are operational. Station Dodewaard is only operational from 2001. The river is relatively straight with an average sinuosity of 1.1 (Julien et al., 2002). The main channel geometry between groynes is relatively constant, with an average main channel width of 280 m (and a standard deviation of 35 m) (Yossef, 2005) which doubles in width near the downstream boundary at Werkendam. The floodplain width varies largely between 500 and 2500 m (Warmink et al., 2011). The river has an average bed slope of $1.05 \cdot 10^{-4}$ m/m.

The river bed mainly consists of sand with a typical grain size D_{50} = 1.0 mm (Wilbers & Ten Brinke, 2003). This corresponds to a Manning roughness value of approximately 0.03 $s \cdot m^{-1/3}$ or a Chézy value of 45 $m^{1/2} \cdot s^{-1}$ (Julien, 2002). In the Waal river dune bed forms are present. These dunes grow in length and height in turn leading to an increasing bed roughness (Julien et. al., 2002; Wilbers & Ten Brinke, 2003). In 1988 and 1999 artificial armoured bed layers at Nijmegen and Sint Andries were constructed to stall erosion of the outer bend. In 1996 submerged groynes at Erlecom were constructed to improve the navigability of ships in the Waal. Additional large-scale interventions for flood risk reduction took place between 2007 and 2017.

The Waal has floodplain compartmentation which is typical for rivers in the Netherlands. This means that there exists a physical man-made barrier (a so-called summer dike) between the main channel and floodplain. Therefore, the water level must exceed the crest level of this barrier to flow into the floodplain. The floodplain compartmentation is modelled as additional flow and storage area in the floodplain (as illustrated in Figure 2) available in the SOBEK 3 modelling program.

The average discharge entering the Waal after the “Pannerdensche Kop” bifurcation is 1500 m^3/s, which is two-third of the Rhine discharge entering The Netherlands at Lobith (Warmink et al., 2011). It typically takes one day for a discharge wave at Pannerdensche Kop to reach the downstream observation station Werkendam.

2.2 *River IJssel*

The upper right panel in Figure 1 presents a geographical overview of the River IJssel. The IJssel is a distributary of the River Rhine in the Netherlands. After the Rhine bifurcates into the Pannerdensch Kanaal, it bifurcates again at the IJsselkop into the IJssel and Nederrijn. The river mouth ends at the IJsselmeer. Therefore, no tidal

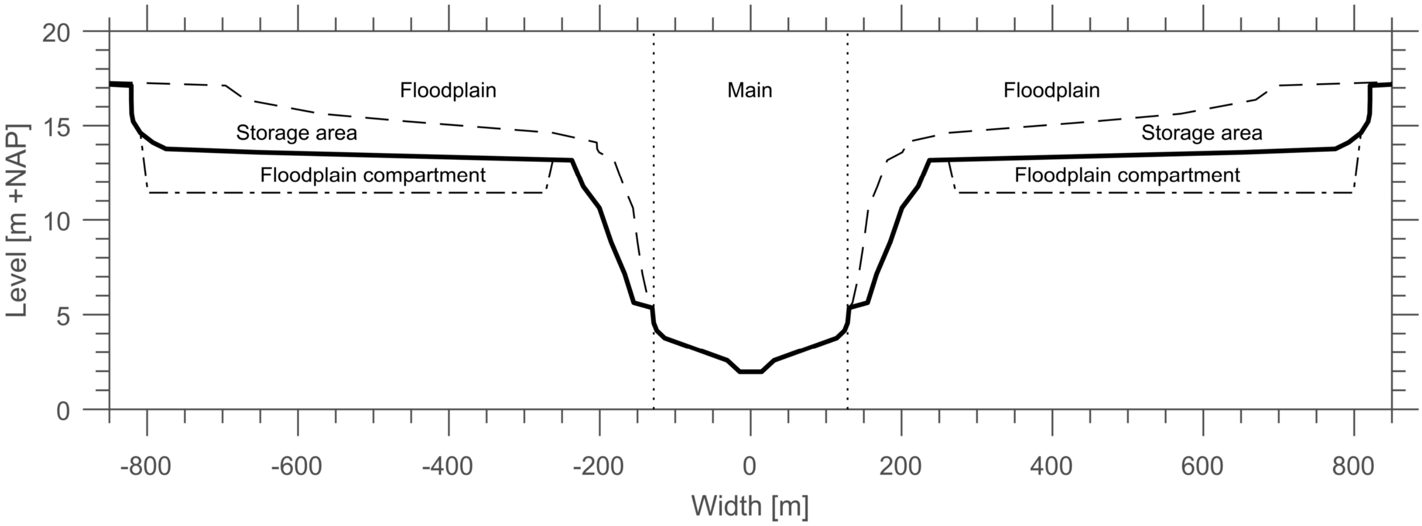

Figure 2. Cross-section profile of the River Waal at river chainage 872.14 km. Storage area is used for modelling groynes and storage due to vegetation in the floodplain. Floodplain compartmentation is modelled as additional flow and storage area in the floodplain.

influence is present at the downstream boundary of the IJssel. However, influence due to wind set-up is present because the IJsselmeer is a large lake.

Along the IJssel, fifteen water level observation stations are operational. Stations Westervoort, De Steeg, Eefde, Deventer, Wijhe were not operational in 1993 and 1995.

The river has a sinuosity of 1.6 due to sharp meandering river bends (as can be seen in Figure 1). Furthermore, the main channel width is roughly 80 m upstream and increases to roughly twice its width downstream. The average floodplain width is roughly 10 times the main channel width (Thonon et al., 2007). The IJssel has floodplain compartmentation (see previous section for more information). The bed slope is slightly smaller than the Waal with $0.83 \cdot 10^{-4}$ m/m. Large-scale interventions for flood risk reduction took place between 2007 and 2017. The river bed mainly consists of sand with a typical grain size D_{50} = 0.5 mm (Wilbers, 1997). Like in the River Waal, river dunes are present in the IJssel.

The average discharge entering the IJssel after the "IJsselkop" bifurcation is 250 m^3/s, which is one-ninth of the Rhine discharge (Thonon et al., 2007). It takes typically one-and-a-half to two days for a discharge wave at IJsselkop to reach the downstream river mouth into the IJsselmeer at Ketel- and Kattendiep.

3 METHOD

3.1 *1D hydrodynamic model*

The Dutch Ministry for Infrastructure and Environment maintains 1D and 2D models for all major Dutch rivers. For this study we use 1D hydrodynamic river models developed in the SOBEK 3 modelling program, because we need small computational times to perform multiple calibration runs.

Three models are used following the calibration and validation periods: winter of 1995 for calibration and winters of 1993 and 2011 for validation. The discharge waves of these periods for the Waal are presented in Figure 3. The Manning roughness formula is used because it is better suited in the use of compound channels (Huthoff & Augustijn, 2004).

3.2 *Location dependency*

The hydraulic roughness along the longitudinal direction of the river can be expressed using multiple roughness trajectories. A roughness trajectory is defined between two observation stations to avoid over-parametrization in the calibration. The roughness value of a trajectory is taken to be uniform along the whole trajectory. Roughness trajectories in the models are correlated to each other because of the subcritical flow in the two Rhine branches. Therefore, downstream effects can propagate upstream. The location dependency is investigated using a varying number of these roughness trajectories of roughly equal length. Five roughness trajectories are possible in the Waal, since there are six observation stations available.

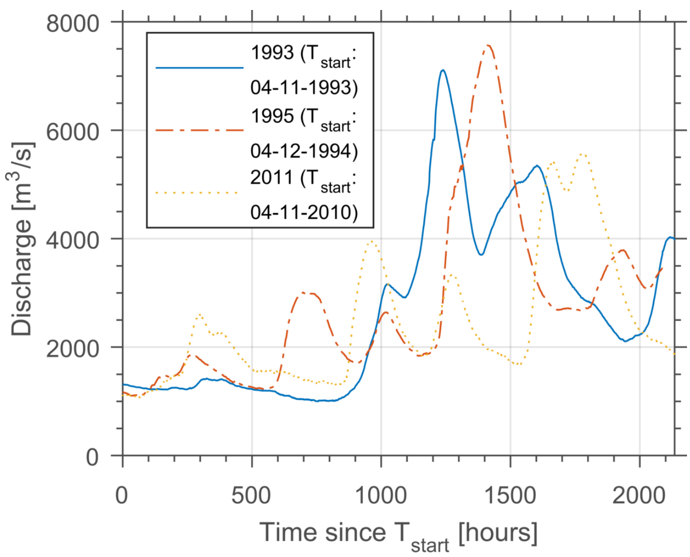

Figure 3. Discharge waves of 1993, 1995 and 2011 for the Pannerdensche Kop location in the River Waal. The discharge waves at the IJsselkop in the River IJssel have the same shape but are roughly three to four times smaller in magnitude.

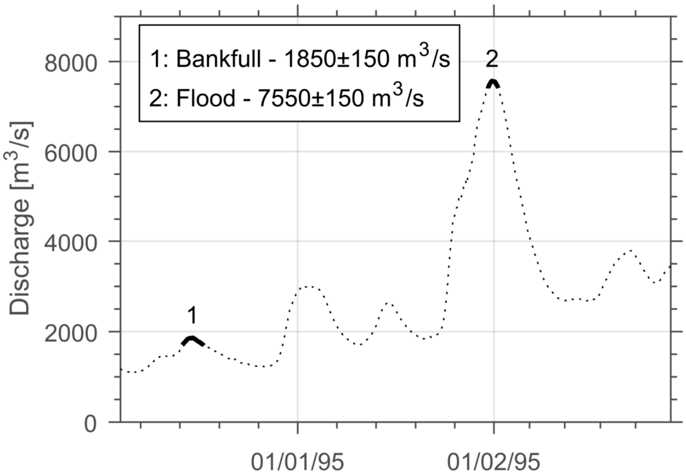

Figure 4. Bankfull and flood stage discharge levels with discharge window used in location dependency calibrations for the River Waal.

Six roughness trajectories are possible in the IJssel, since there are seven observation stations available. The observation station at the downstream boundary is excluded because the water level observation data of this station is used as the downstream boundary condition. For the IJssel this means the observation stations Ketelhaven, Ramspolbrug and Kamperhoek are not included in the calibration.

We vary the number of trajectories with $N = [1,2,4,5]$ for the Waal and with $N = [1,2,3,5,6]$ for the IJssel. To investigate the location dependency for different discharge stages, two discharge stages are calibrated (as illustrated in Figure 4 for the Waal): 1) bankfull stage and 2) flood stage. Only the top of the peak is considered where the water level is roughly constant. Therefore, a discharge window around the discharge levels is applied. The placement of the discharge levels and windows of each trajectory is adjusted according to the propagation of the discharge wave from up- to downstream boundary because of diffusion of the wave and lateral discharge sources along the river length.

3.3 *Discharge dependency*

The calibration discharge stage is referred to as a discharge level. The discharge dependency is investigated using a varying number of discharge levels. The hydraulic roughness coefficient is described by an empirical linear tabular function dependent on the discharge. We vary the number of these discharge levels evenly over the discharge range with $N = [2,3,4,6,8,12]$ for both the Waal and the IJssel. For the Waal, the minimum discharge level is fixed at 1000 and the maximum at 8000 m^3/s. For the IJssel, the minimum discharge level is fixed at 200 and the maximum at 1900 m^3/s. The minimum and maximum are slightly lower/higher than the minimum and maximum discharge of the 1995 discharge wave (as presented in Figure 3). This is because of the tidal influence at the downstream boundary of the Waal and wind set-up at the downstream boundary of the IJssel which create small fluctuations in discharge. All discharge levels are calibrated in one calibration run. The whole three-month time period of the discharge wave is used for calibration together with the maximum of five roughness trajectories for the Waal and with the maximum of six trajectories for the IJssel.

3.4 *Calibration procedure*

Different configurations in roughness trajectories and discharge levels are applied in the calibration to obtain different calibrated roughness values. The 1995 discharge wave of the Rhine is used as the calibration period (as illustrated in Figure 2). We use all observation data for every calibration run.

The software package OpenDA is used to automatically calibrate the model with the DuD optimization algorithm (Ralston & Jennricht, 1978) and a weighted nonlinear least squares objective function:

$$Q(\theta) = \frac{1}{2}\sum_{i=1}^{k}\sum_{j=1}^{l}\frac{1}{\sigma^2}\left(y_{i,j} - \hat{y}_{i,j}(\theta)\right)^2 \quad (1)$$

where Q = objective value; θ = set of parameters; k = number of observation stations; l = number of observed water levels; σ = observation uncertainty; y = observed water level; and ŷ = predicted water level.

3.5 *Validation*

Validation is performed to identify which calibrated roughness provides the best water level predictions and is performed on the whole three-month time period of the 1995 discharge wave and the two other discharge waves of 1993 and 2011 (as illustrated in Figure 2). The discharge wave of 1993 is chosen as it closely resembles the 1995 discharge wave. The 2011 discharge wave is chosen as it very different from the 1995 discharge wave but still provides a large discharge range. Moreover, the river geometry in 2011 has changed significantly compared to 1995 due large-scale interventions for flood risk reduction.

The RMSE criterion is used for validation because of the mathematical similarity with the used objective function for calibration. The whole time period of the discharge wave is used for validation. The RMSE-criterion is slightly adapted by adding a weighing factor γ to account for the more frequent low water levels and less frequent high water levels:

$$RMSE = \sqrt{\frac{1}{k \cdot l}\sum_{i=1}^{k}\sum_{j=1}^{l}\gamma_{i,j} \cdot \left(y_{i,j} - \hat{y}_{i,j}\right)^2} \quad (2)$$

where y = simulated water levels; ŷ = observed water levels; γ = weighting factor; l = number of observed water levels of one observation location; and k = number of observation stations. The adaptation of the RMSE criterion is needed because the water level prediction accuracy of the used models should be equal across the whole water level range. The weighting factor γ is determined by dividing a uniform water level histogram by the histogram

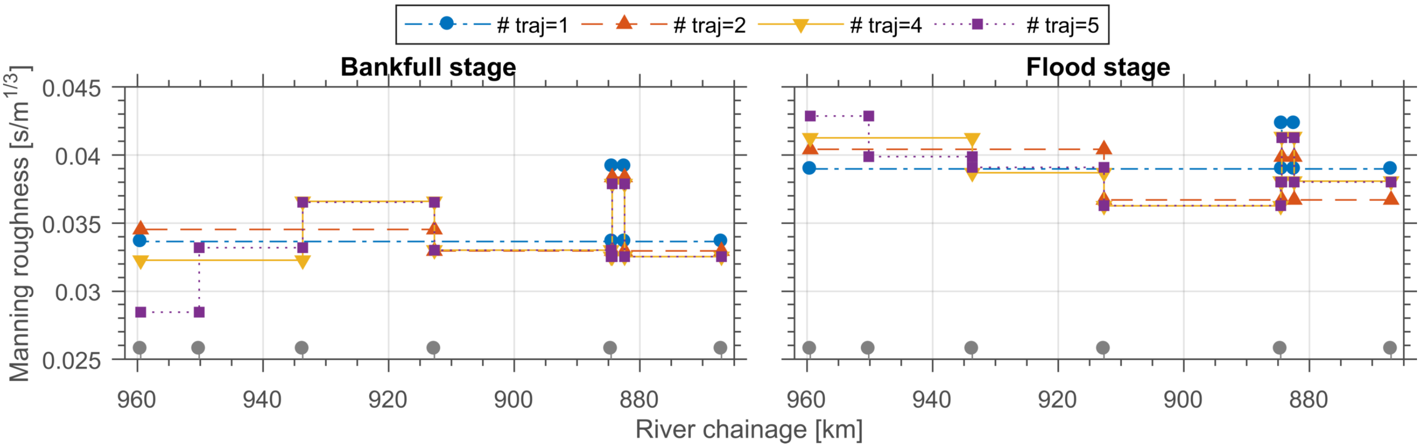

Figure 5. Calibrated roughness for varying number of roughness trajectories and for both bankfull and flood stage discharge level for the River Waal. The grey dots right above the x-axis shows observation station locations.

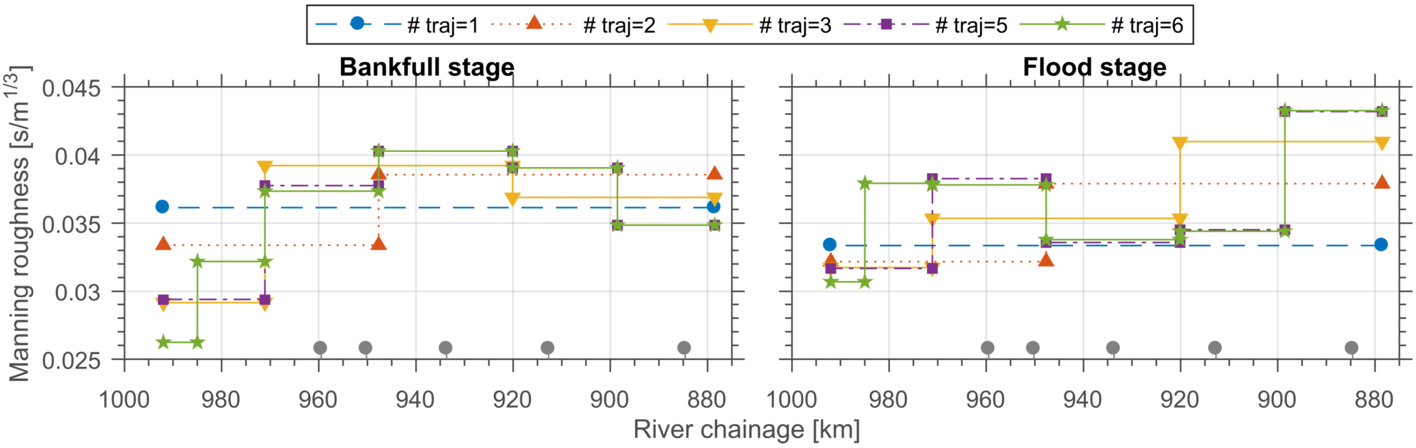

Figure 6. Calibrated roughness for varying number of roughness trajectories and for both bankfull and flood stage discharge level for the River IJssel. The grey dots right above the x-axis shows observation station locations.

based on observations. The bin size of the histogram based on observations is based on Freedman-Diaconis rule (as summarized by Izenmann (1991)).

4 RESULTS: CALIBRATED ROUGHNESS

4.1 *Calibrated roughness location dependency*

Figure 5 and 6 presents the calibrated roughness for both bankfull and flood stage discharge levels for varying number of roughness trajectories for the Waal and IJssel. The increase in roughness at river kilometre 882 in Figure 5 for the Waal is due to the artificial armoured bed layer at Nijmegen.

For both rivers the calibrated roughness for the flood stage is overall higher than for the bankfull stage. This is a result of floodplain compartmentation (and can be classified as a model error) or the result of the growth of river dunes. It is unclear which contribution (i.e. floodplain compartmentation or river dune growth) is more dominant.

The roughness difference near the downstream boundary in Figure 5 for the Waal, starting from river kilometre 933, is possibly the result of an incorrect boundary condition. The backwater effect induced by the boundary condition, under- or overestimates the water level at observation point Vuren at river kilometre 950. Calibration compensates for this by decreasing or increasing the roughness depending on the used discharge level.

Figure 6 shows a large roughness decrease for the flood stage discharge level between river kilometre 889 and 942 km for the IJssel for five and six trajectories. This decrease is a result of the overestimation of water levels in sharp bends. Bank overflow in these bends occur, however this is difficult to accurately model in 1D. Calibration compensates for this overestimation by lowering the roughness.

4.2 *Calibrated roughness discharge dependency*

Figure 7 and 8 presents the calibrated roughness-discharge functions for the five roughness trajectories for the Waal and for the six roughness trajectories for the IJssel for $N = [2,4,6,8]$ discharge levels. Overall, the calibrated roughness in both rivers increases as the discharge increases. The roughness decrease between river kilometer 889 and 942 km in the IJssel (see Figure 8) is a result of overestimation of water levels due to bank overflow in sharp river bends (see previous section for more information). Moreover, more details appear if more discharge levels are calibrated.

These details show at low discharge a sharp roughness increase, after which it decreases again for the Waal. This decrease is not clearly visible for the IJssel because of two

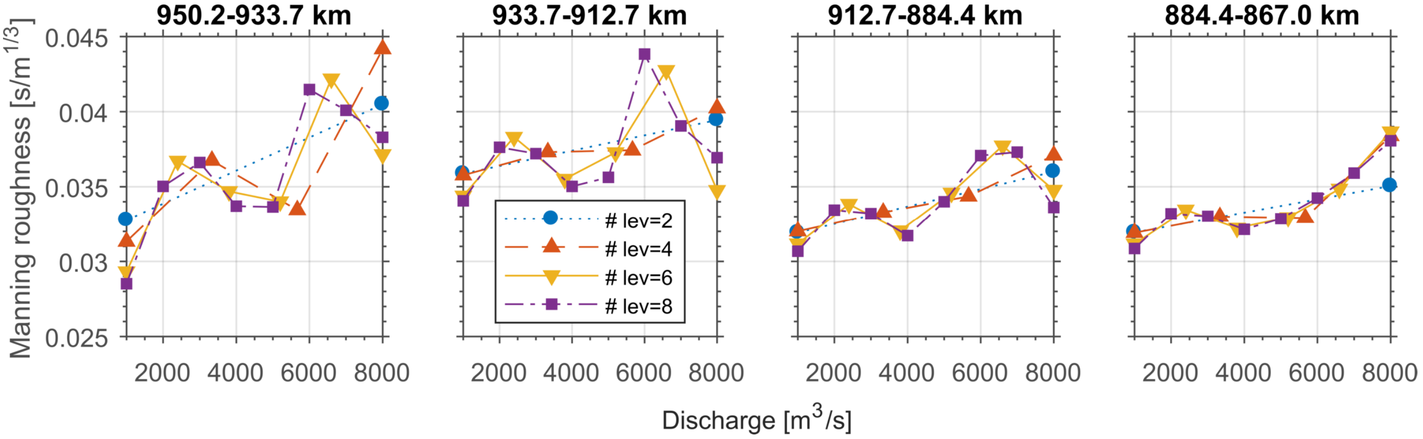

Figure 7. Calibrated roughness-discharge functions for varying number of discharge levels for the River Waal. From right to left plots show the functions from upstream to downstream sections between measurement stations. The most downstream section is not shown, because results are largely affected by the downstream boundary condition.

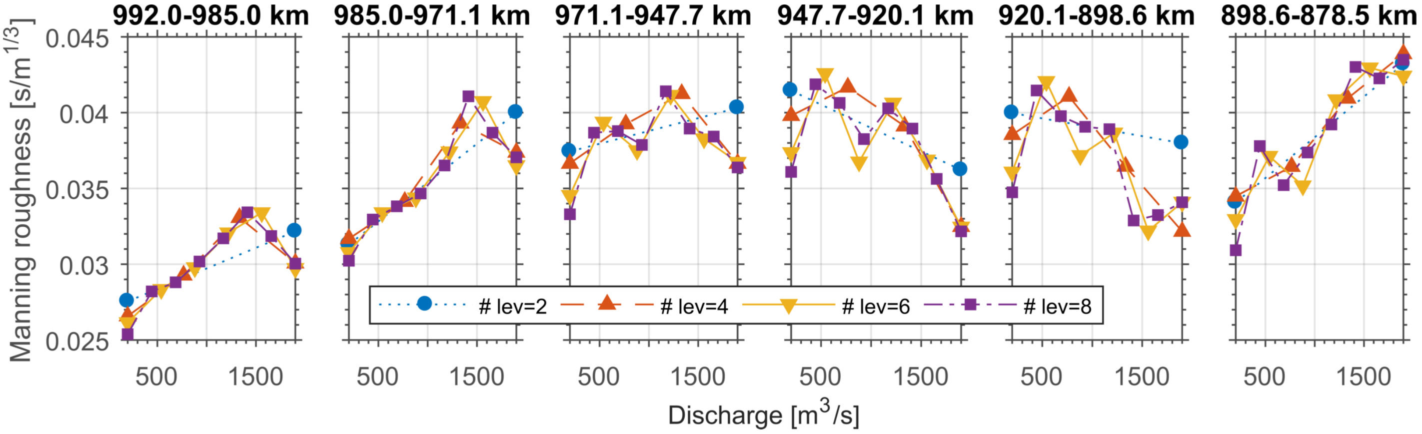

Figure 8. Calibrated roughness-discharge functions for varying number of discharge levels for the River IJssel. From right to left plots show the functions from upstream to downstream sections between measurement stations.

reasons. First, the overestimation of water levels due to bank overflow in sharp river bends. Second, the main channel width increases downstream to twice the upstream width. This results in a transition from bankfull to flood stage at a higher discharge (see next paragraph for explanation). After the roughness decrease it shows a high roughness peak.

The first roughness increase at low discharge is expected as river dunes grow increasing the bed roughness in the main channel in turn. However, the roughness decrease and peak at higher discharge cannot be explained by bed-form dynamics.

The roughness decrease can be attributed to the transition from bankfull stage (only main channel roughness affects compound roughness) to flood stage (both main channel and floodplain roughness affect compound roughness). During this transition the hydraulic radius decreases suddenly (as presented in Figure 9). The drop in hydraulic radius results in a lower roughness in the compound channel roughness calculation defined by:

$$C = \frac{\sqrt[6]{R_m}}{n_m}\frac{A_m}{A_t}\sqrt{\frac{R_m}{R_t}} + C_f\frac{A_f}{A_t}\sqrt{\frac{R_f}{R_t}} \qquad (3)$$

where C = compound Chezy; R_m = main channel hydraulic radius; n_m = main channel Manning; A_m = main channel flow area; A_t = total flow area; R_t = total hydraulic radius; C_f = floodplain Chezy; A_f = floodplain flow area; and R_f = floodplain hydraulic radius. A higher Chezy value means a lower roughness.

At the start of the transition the floodplain area is still small compared to the main channel. The contribution of the second term in Eq. 3 is therefore small. Furthermore, the compound roughness is mostly affected by the hydraulic radius ratio because the total flow area almost equals the main channel flow area at the beginning of the transition (i.e. $A_m/A_t \approx 1$). If the floodplain flow area is large enough, the contribution of the floodplain roughness becomes bigger.

However, as the calibrated roughness indicates, this lower compound roughness is not low enough for predicting the observations accurately. Therefore, the calibrated main channel roughness is lowered too. At trajectory Vuren-Hardinxveld (950 till 960 km) the roughness decrease is less apparent because the main channel width increases to twice the main channel width upstream. Therefore, the contribution of the main channel roughness to the compound roughness is much larger.

The roughness peak (around 6000 m^3/s in Figue 7 and around 1500 m^3/s in Figure 8) is a result of the compartmentation of the floodplain. The compartmentation is modelled using a specific model feature available in the SOBEK 3 modelling program. In reality during the large discharge peak of 1995, openings

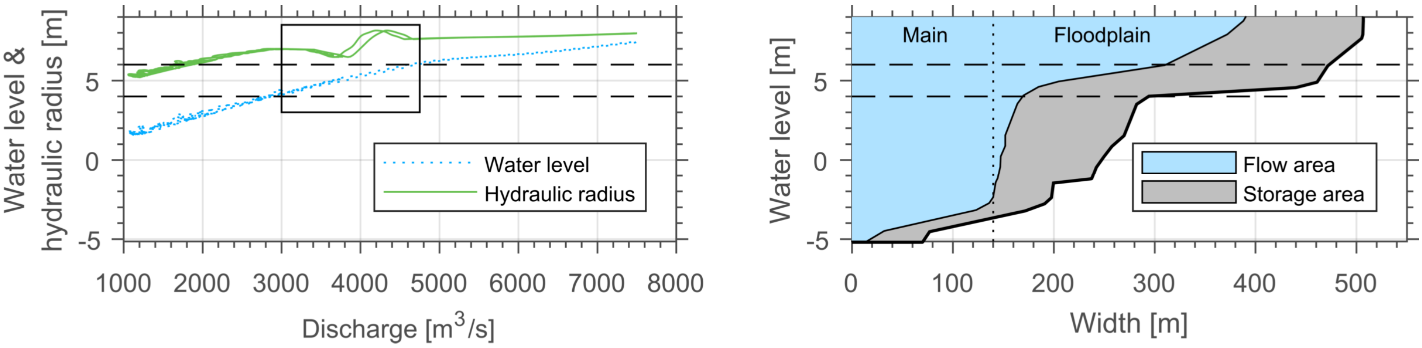

Figure 9. Water level and hydraulic radius at location Zaltbommel (935 km) in the River Waal compared to the symmetric cross-section profile. Transition zone of bankfull to flood stage indicated by dashed line. Transition from bankfull to flood stage influences hydraulic radius as indicated by the lines in the rectangle in the right panel.

in the barrier creating the compartmentation (i.e. summer dike) are opened. This creates a discrepancy between the predictions and observations for which the calibrated roughness compensates. However, as the calibrated roughness still increases overall with increasing discharge, it is believed that the growth of river dunes is still present in the calibrated roughness. However, as indicated in the previous section, it is unclear which effect (i.e. floodplain compartmentation or river dune growth) is more dominant in the calibration.

5 RESULTS: VALIDATION

5.1 *Location dependency validation*

Figure 10 presents the validation results of the location dependent cases for the Waal and IJssel. The results of all three bankfull cases for the Waal show a clear minimum RMSE (and thus the most accurate water level predictions) when using two roughness trajectories. This corresponds to roughly a roughness trajectory length of 40 km. However, for the flood cases no minimum RMSE is present. In these three cases increasing the number of roughness trajectories also increases the accuracy of the water level predictions. Still, the flood 2011 case shows no strong improvement if increasing the number of roughness trajectories beyond two. Therefore, it is unclear which number of roughness trajectories produces a minimum error between water level predictions and observations when the whole water level range is considered equally important for the prediction accuracy of the model.

The results of the IJssel on the other hand show a clear minimum RMSE for the flood stage cases when using three roughness trajectories. This corresponds to roughly a roughness trajectory length of 45 km. However, for all three bankfull cases no clear minimum RMSE is present.

When both conclusions of the Waal and IJssel are combined, it can be argued there exists some minimum number of roughness trajectories with a length of roughly 40 to 45 km.

5.2 *Discharge dependency validation*

Figure 11 presents the validation results of the discharge dependent cases for the Waal and IJssel. The RMSE of all instances are lower than their counterparts in the location dependent cases for all number of roughness trajectories (see Figure 10). Making the hydraulic roughness coefficient a function of the discharge with two discharge levels already results in more accurate water level predictions than all location dependent cases. Therefore, it can be concluded that accuracy of water level predictions depends more on the number of discharge levels than on the number of roughness trajectories.

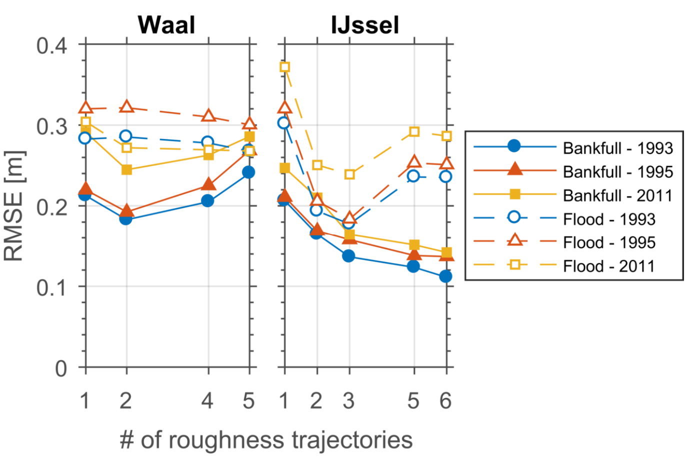

Figure 10. Validation of location dependent calibrations for the Waal and IJssel

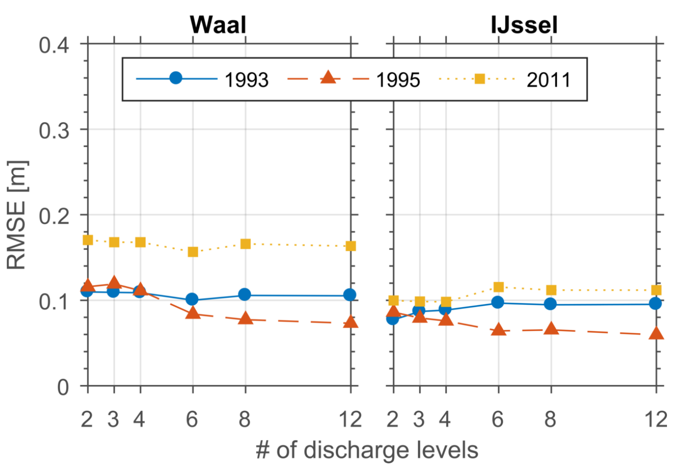

Figure 11. Validation of discharge dependent calibrations for the Waal and IJssel

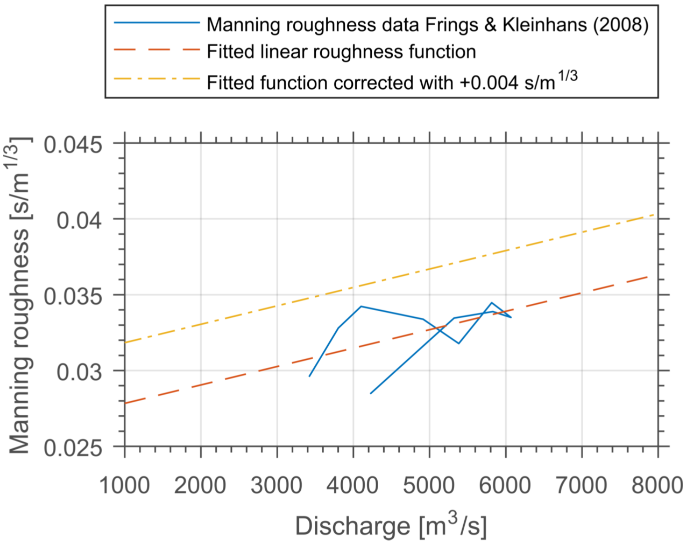

Figure 12. Measured Manning roughness data of Frings & Kleinhans (2008) with fitted linear function and a corrected fitted linear function with +0.004 s/m$^{1/3}$

Both the 1993 and 2011 cases for the Waal show a minimum RMSE value and therefore the most accurate water level predictions at six discharge levels. This corresponds to the calibrated roughness-discharge function where the transition from bankfull to flood stage and the floodplain compartmentation are captured. However, improvement in accuracy of water level predictions between two and six discharge levels is roughly 9% and thus minimal.

There is no clear minimum number of discharge levels visible for the IJssel. However, 2, 3 or 4 levels produce roughly the same lowest RMSE and therefore these three configurations can be viewed as the minimum number of discharge levels. This minimum number of discharge levels is different from the Waal, because the calibrated roughness-discharge functions vary greatly per roughness trajectory (as can be seen in Figure 8) compared to the functions of the Waal which show a distinct shape for each trajectory (as can be seen in Figure 7).

6 DISCUSSION

The results show that the calibrated hydraulic roughness coefficient mostly depends on the discharge. The calibrated values show the largest value range for the discharge. The location dependency is mostly a result of an incorrect downstream boundary. The roughness trajectory between TielWaal and Zaltbommel (913 till 933 km) shows a strong roughness increase for the bankfull stage discharge level compared to the other trajectories. It is unknown why this happens.

The calibration and validation results are based on two case studies. Apart from the presented results, one other case study with a more recent Waal model have been performed. The results of this case study are similar to the ones presented.

The calibrated roughness at higher discharges is largely influenced by the floodplain compartmentation.

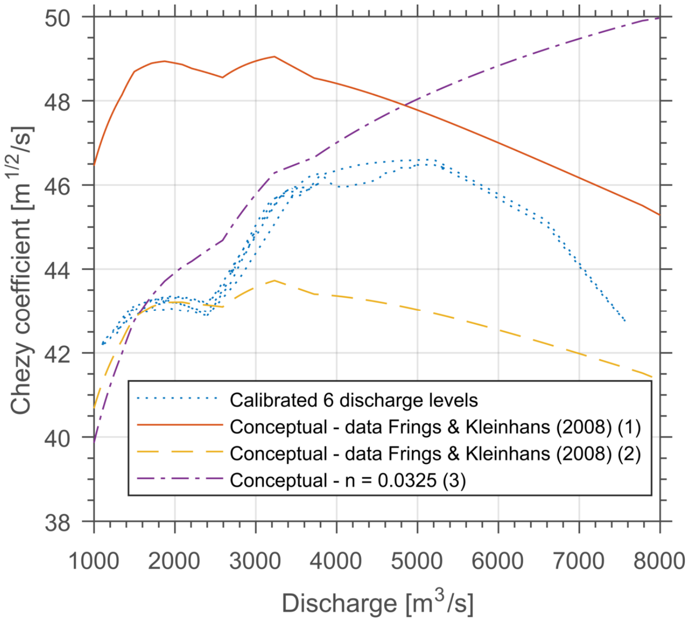

Figure 13. Chezy values from calibrated model and conceptual model as function of discharge for Pannerdensche Kop location. Conceptual model (1) uses a linear discharge dependent main channel Manning roughness function fitted on the data of Frings & Kleinhans (2008), (2) extends (1) by correcting the fitted function with +0.004 s/m$^{1/3}$ and (3) uses a constant main channel Manning roughness

Therefore, it remains unclear whether the overall roughness increase for the whole discharge range is an indicator for the growth of river dunes. It is advised to perform this study with a river similar to the Waal or IJssel but where no compartmentation of the floodplain is present. This proposed study could help aid in the development of roughness prediction models based on river bed forms (e.g. Paarlberg et al. (2010)).

6.1 *Conceptual discharge dependent roughness model*

When the effect of floodplain compartmentation on the calibrated roughness is not considered, the calibrated roughness-discharge functions show a distinct shape. This distinct shape could be captured by a conceptual roughness model that is only discharge dependent. A start of this conceptual model is proposed for the Waal by combining the increasing roughness because of river dune growth and the compound roughness calculation method (Eq. 3).

We model the main channel Manning roughness as a linear function of the discharge using measured Manning roughness data of the Waal from Frings & Kleinhans (2008) obtained during a discharge peak in the winter of 1998 (solid line in Figure 12). The measured Manning roughness data are obtained near the Pannerdensche Kop location and contain hysteresis effects which are not considered in the conceptual model. The floodplain roughness is modelled as a logarithmic function based on the modelled floodplain roughness in the 1995 model.

We compare the calculated compound Chezy values of this conceptual model (solid line in Figure 13) with the calculated compound Chezy values from the calibration

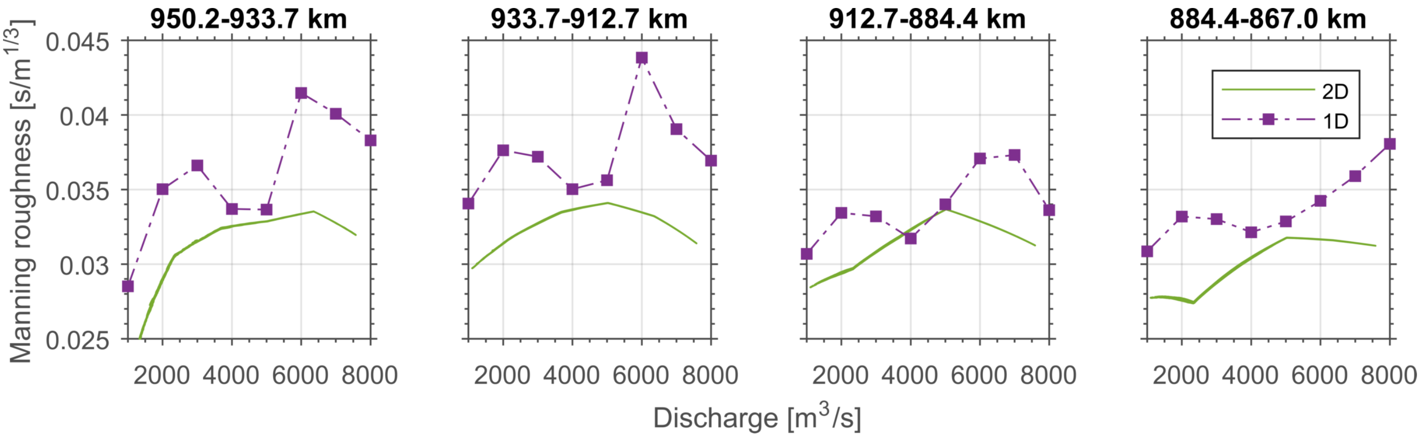

Figure 14. Calibrated roughness-discharge functions with six discharge levels for 2D calibration of the River Waal compared to 1D calibration. From right to left plots show the functions from upstream to downstream sections between measurement stations. The most downstream section is not shown, because results are largely affected by the downstream boundary condition. The Manning roughness of the 2D calibration is calculated with Eq. 4 and $n = \sqrt[6]{h}/C$ using the calibrated α-values and water depth.

using six discharge levels for the Waal at the Pannerdensche Kop location (dotted line in Figure 13). The compound Chezy values using one constant Manning value of 0.0325 s/m$^{1/3}$ are presented too (dash-dot line in Figure 13). To better fit the compound Chezy values obtained from calibration, the conceptual model using a linear Manning-discharge function is corrected with +0.004 s/m$^{1/3}$ (dashed line in Figure 13).

Comparison between the conceptual models shows that using a linear Manning-discharge function for the main channel provides a good start for a conceptual discharge dependent roughness model. At higher discharges the conceptual model shows some discrepancies. This can be attributed to the large influence of the floodplain roughness at this stage and the linear nature of the main channel roughness function. Moreover, the data of Frings & Kleinhans (2008) is scarce and the extrapolation of this data is therefore highly uncertain.

6.2 *Calibration of a 2D model*

All the results presented in this paper are obtained with 1D models. However, as 2D models are commonly used too, it is interesting whether the 1D results are representative for the 2D results. Therefore, one calibration with a 2D Waal model using the 1995 discharge wave is performed. We use a simplified version of the Van Rijn roughness height predictor (van Rijn, 1984) in conjunction with the White-Colebrook formula:

$$C = 18\log^{10}\left(\frac{12h}{k_N}\right) \text{ with } k_N = \alpha h^{0.7}\left(1 - e^{-\beta h^{-0.3}}\right) \quad (4)$$

where C = Chezy value; h = water depth at a 2D grid cell; k_N = Nikuradse roughness height; α = calibration parameter; and β = calibration parameter.

The 2D model is calibrated on six discharge levels (i.e. the same from the 1D case) where the α parameter is calibrated. The β parameter is set constant to 2.5 m$^{0.3}$.

Figure 14 presents the calibrated roughness values converted to the Manning coefficient for the 2D Waal case compared to the 1D calibrated roughness values. The 2D calibrated roughness-discharge functions are lower and do not show the transition from bankfull to flood stage and the effect of floodplain compartmentation compared to the 1D calibrated roughness-discharge functions. This is because in 2D the transition from bankfull to flood stage and floodplain compartmentation are modelled more accurately. Therefore, the 2D calibration shows a more apparent increasing roughness with increasing discharge. Furthermore, it supports the idea of roughness prediction models based on river bed forms (e.g. Paarlberg et al. (2010)).

7 CONCLUSION

The location and discharge dependency of the calibrated main channel roughness expressed by the Manning coefficient is studied using two case studies on the River Waal and IJssel in the Netherlands. The results show that the calibrated main channel roughness is mostly dependent on the discharge. Increasing roughness due to river dune growth can be observed at lower discharges. During the transition from bankfull to flood stage a roughness decrease is observed to compensate for model deficiencies. And at higher discharges a roughness peak occurs due to the floodplain compartmentation. At some roughness trajectories in the IJssel model the calibrated roughness decreases with increasing discharge. This is due to the incorrectly modelled bank overflow in sharp river bends. However, as the calibrated roughness increases overall for both the Waal and IJssel with increasing discharge, it is believed that the effect of river dune growth is also present in the calibrated roughness at higher discharges. In case of the location dependency, the difference in roughness values can mostly be attributed to an incorrect downstream boundary condition.

Validation results confirms that the calibrated main channel roughness is mostly discharge dependent. The calculated RMSE values of the location dependency calibrations show a large difference between the used discharge stage (i.e. bankfull or flood). These values are also higher than the RMSE values of the discharge dependency calibrations.

Based on that the main channel roughness is mostly discharge dependent and it shows distinct features, we propose a start of a conceptual discharge dependent roughness model. Furthermore, one calibration run with a 2D model has been performed. The calibrated roughness-discharge functions of this calibration show an increasing roughness with increasing discharge. However, they do not show the transition from bankfull to flood stage and the effect of floodplain compartmentation compared to the 1D calibrated roughness-discharge functions. Therefore, the effect of increasing roughness due to growing river dunes is present in the calibrated roughness values.

ACKNOWLEDGEMENTS

This study was conducted at Deltares, and facilitated by the University of Twente. It is part of the RiverCare research programme, supported by the Dutch Technology Foundation TTW (project-number 13520), which is part of the Netherlands Organisation for Scientic Research (NWO), and which is partly funded by the Ministry of Economic Affairs under grant number P12-14 (Perspective Programme).We would also like to thank Rijkswaterstaat for providing the models and observation data.

REFERENCES

Bates, P. D., Horritt, M. S., Aronica, G., & Beven, K. J. (2004). Bayesian updating of flood inundation likelihoods conditioned on flood extent data. Hydrological Processes, 18(17), 3347–3370.

Best, J. (2005). The fluid dynamics of river dunes: A review and some future research directions. Journal of Geophysical Research: Earth Surface, 110(F4), 1–21.

Frings, R. M., & Kleinhans, M. G. (2008). Complex variations in sediment transport at three large river bifurcations during discharge waves in the river Rhine. Sedimentology, 55(5), 1145–1171.

Hall, J. W., Tarantola, S., Bates, P. D., & Horritt, M. S. (2005). Distributed Sensitivity Analysis of Flood Inundation Model Calibration. Journal of Hydraulic Engineering, 131(2), 117–126.

Huthoff, F., & Augustijn, D. (2004). Channel roughness in 1D steady uniform flow: Manning or Chézy? In Proceedings NCR-days 2004 (pp. 98–100).

Izenman, A. J. (1991). Recent developments in nonparametric density estimation. Journal of the American Statistical Association, 86(413), 205–224.

Julien, P. Y. (2002). River Mechanics. Cambridge University Press.

Julien, P. Y., Klaassen, G. J., Ten Brinke, W. B. M., & Wilbers, A. W. E. (2002). Case Study: Bed Resistance of Rhine River during 1998 Flood. Journal of Hydraulic Engineering, 128(12), 1042–1050.

Paarlberg, A. J., Dohmen-Janssen, C. M., Hulscher, S. J. M. H., Termes, P., & Schielen, R. (2010). Modelling the effect of time-dependent river dune evolution on bed roughness and stage. Earth Surface Processes and Landforms, 35(15), 1854–1866.

Pappenberger, F., Beven, K. J., Horritt, M. S., & Blazkova, S. (2005). Uncertainty in the calibration of effective roughness parameters in HEC-RAS using inundation and downstream level observations. Journal of Hydrology, 302(1–4), 46–69.

Ralston, M. L., & Jennricht, R. I. (1978). Dud, A Derivative-Free Algorithm for Nonlinear Least Squares. Technometrics, 20(1), 7–14.

Thonon, I., Middelkoop, H., & van der Perk, M. (2007). The influence of floodplain morphology and river works on spatial patterns of overbank deposition. Netherlands Journal of Geosciences, 86(1), 63–75.

van Rijn, L. C. (1984). Sediment Transport, Part III: Bed forms and Alluvial Roughness. Journal of Hydraulic Engineering, 110(12), 1733–1754.

Vidal, J.-P., Moisan, S., Faure, J.-B., & Dartus, D. (2007). River model calibration, from guidelines to operational support tools. Environmental Modelling & Software, 22(11), 1628–1640.

Warmink, J. J. (2011, September 2). Unraveling uncertainties. University of Twente, Enschede, The Netherlands.

Warmink, J. J., Booij, M. J., van der Klis, H., & Hulscher, S. J. M. H. (2007). Uncertainty in water level predictions due to various calibrations. In CAIWA (pp. 1–18).

Warmink, J. J., van der Klis, H., Booij, M. J., & Hulscher, S. J. M. H. (2011). Identification and Quantification of Uncertainties in a Hydrodynamic River Model Using Expert Opinions. Water Resources Management, 25(2), 601–622.

Wilbers, A. W. E. (1997). De bodemsamenstelling van Waal en IJssel in de jaren 1966, 1976, 1984 en 1995: RIZA rapport 97.009. Arnhem: Rijkswaterstaat.

Wilbers, A. W. E., & Ten Brinke, W. B. M. (2003). The response of subaqueous dunes to floods in sand and gravel bed reaches of the Dutch Rhine. Sedimentology, 50(6), 1013–1034.

Yossef, F. M. (2005). Morphodynamics of Rivers with Groynes.